Supplement: Tropical forcing of increased Southern Ocean climate variability revealed by a 140-year subantarctic temperature reconstruction

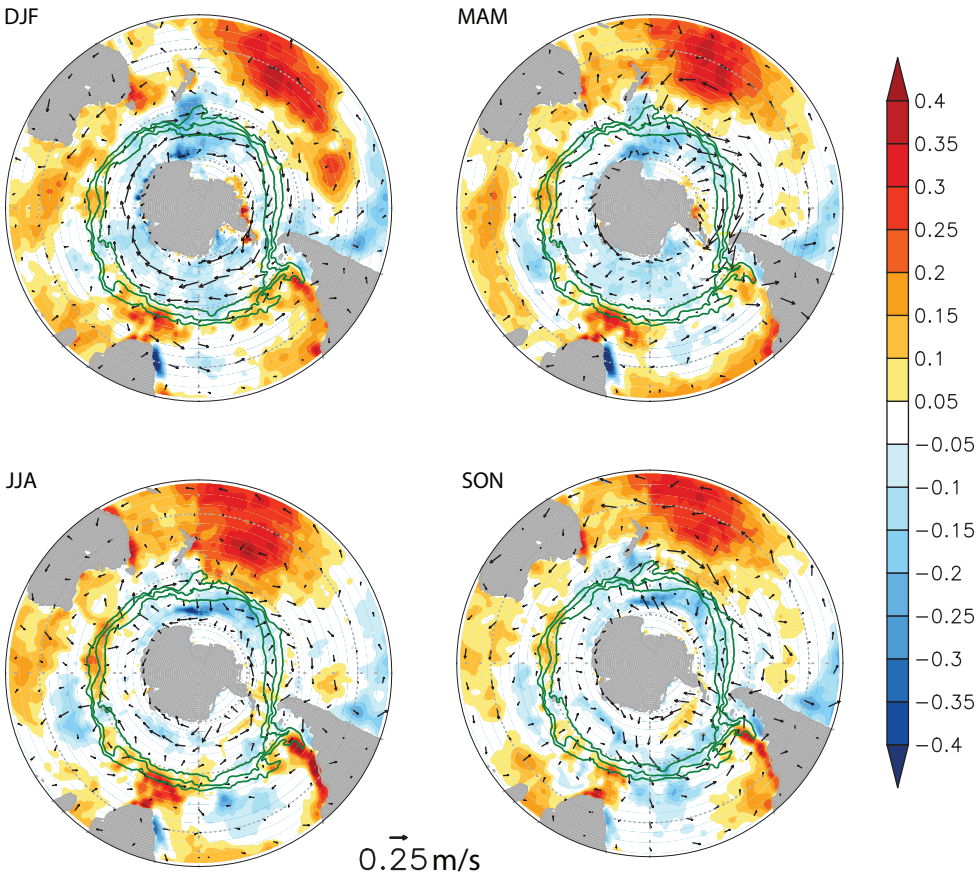

Figure S1: Trends in austral sea surface temperature (SST; shading) and 925-hPa winds (vectors) for December-February (DJF), March-May (MAM), June-August (JJA) and September-November (SON) since 1979. Overlaid in green are the main fronts of the Antarctic Circumpolar Current (Sallée et al., 2012).

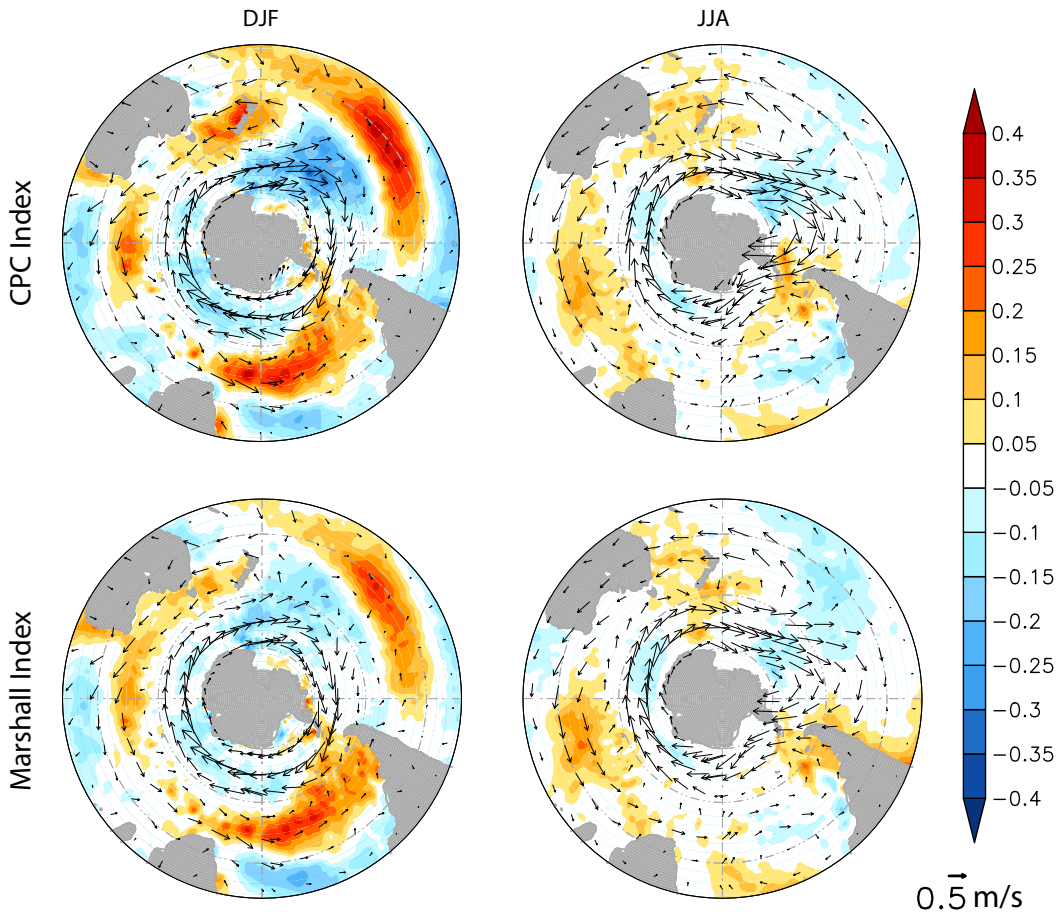

Figure S2: Austral summer (December-February) and winter (June-August) mean regressions of sea surface temperature (SST) and 925-hPa winds (vectors) onto different indices of the Southern Annular Mode (SAM) since 1979: the Climate Prediction Centre (CPC) (http://www.cpc.ncep.noaa.gov/products/precip/CWlink/daily_ao_index/aao/aao.shtml) and Marshall (2003).

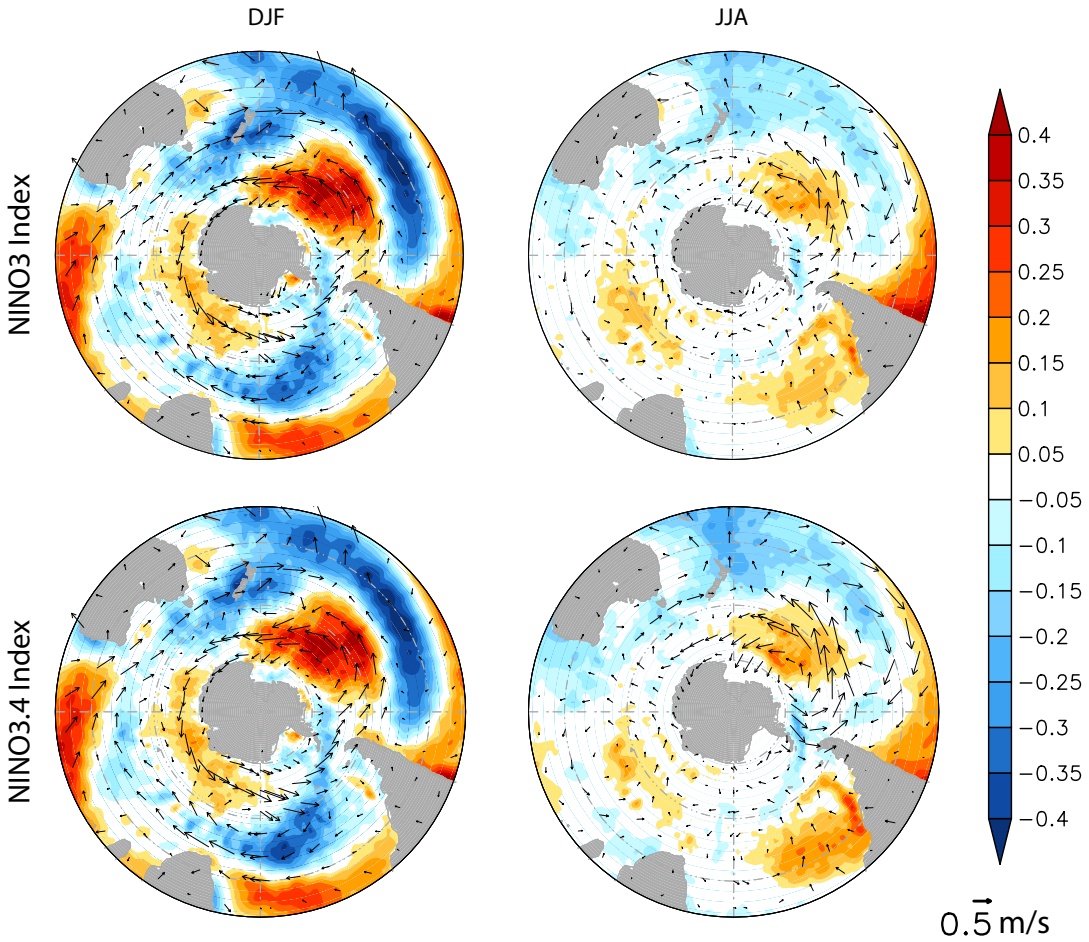

Figure S3: Austral summer (December-February) and winter (June-August) mean regressions of sea surface temperature (SST) and 925-hPa winds (vectors) onto the Nino 3 and Nino 3.4 regions of the El Niño-Southern Oscillation since 1979.

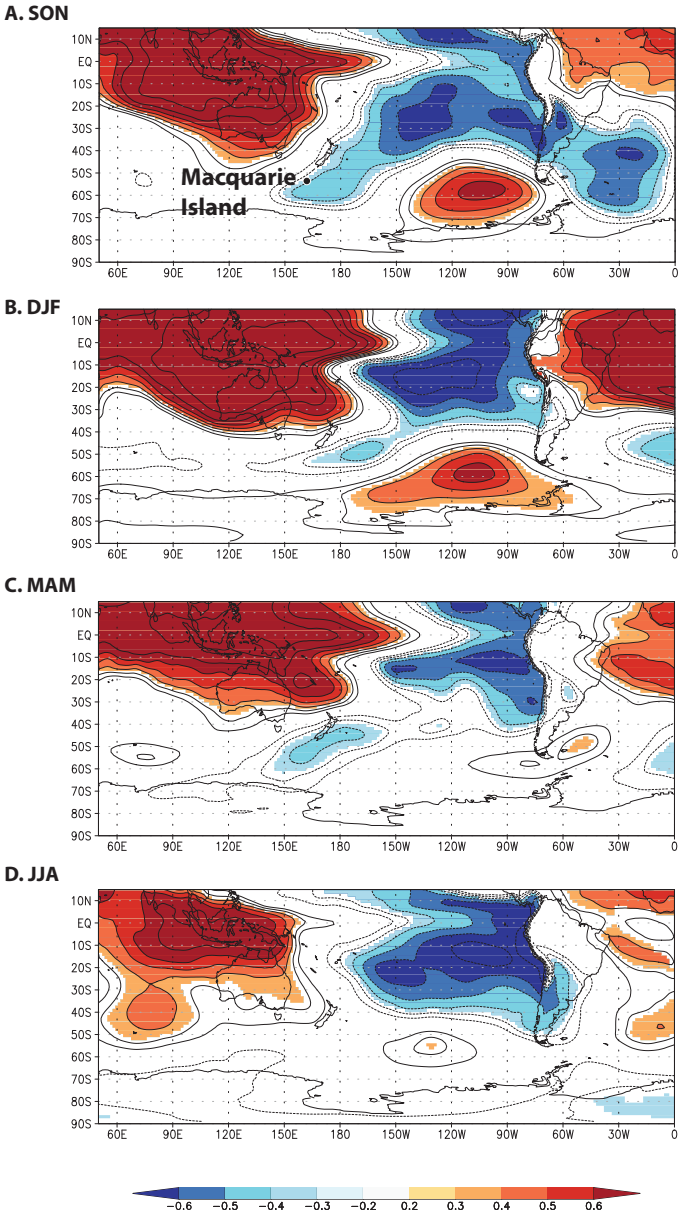

Figure S4: Spatial correlation between detrended and deseasonalised Nino 3 sea surface temperature (Rayner et al., 2003) and 850 hPa height anomalies for September-November (SON) (**A.**), December-February (DJF) (**B.**), March-May (MAM) (**C.**), and June-August (JJA) (**D.**) using ERA Interim (Dee et al., 2011) for the period 1979-2015. Significance $p_{field} < 0.05$. Note: the tropical teleconnection is most strongly expressed at high latitudes during the austral spring and summer.

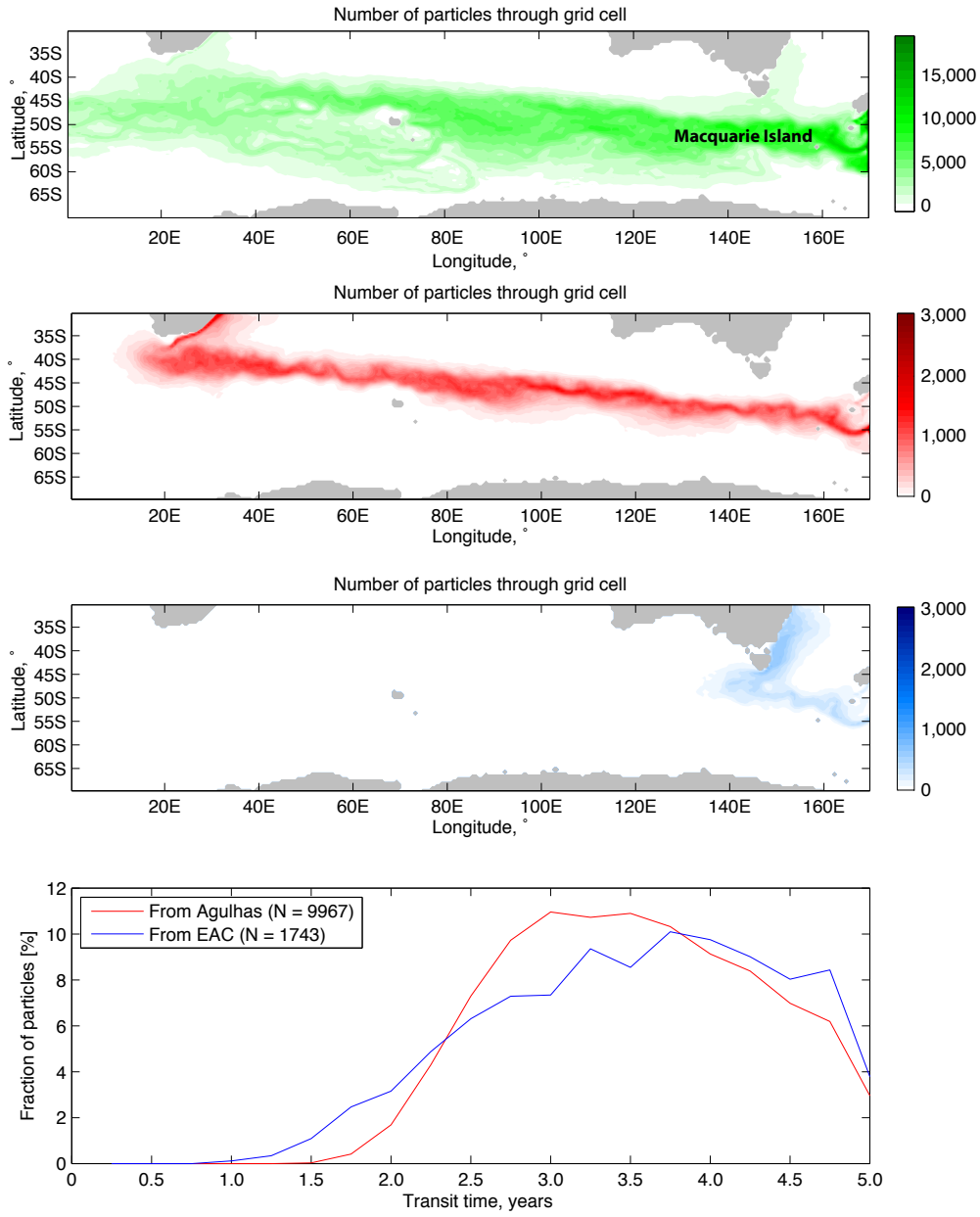

28

29 **Figure S5:** Reverse pathway of the Antarctic Circumpolar Current (A.), Agulhas (B.)

30 and East Australian (C.) current particles that reach the southwest subantarctic region

31 east of 170˚E and south of 45˚S and transit time (D.). Note that the color axis for the

32 number of particles in Panel A. is different to Panels B. and C. Analysis undertaken

33 using Lagrangian particles in the eddy-resolving Japanese Ocean model For the Earth

34 Simulator (OFES) (Masumoto et al., 2004).

35

36 **Figure S6:** Area under the graph calculated from monthly mean temperatures obtained from

37 Macquarie Island and expressed relative to the AAE period (1912-1915).

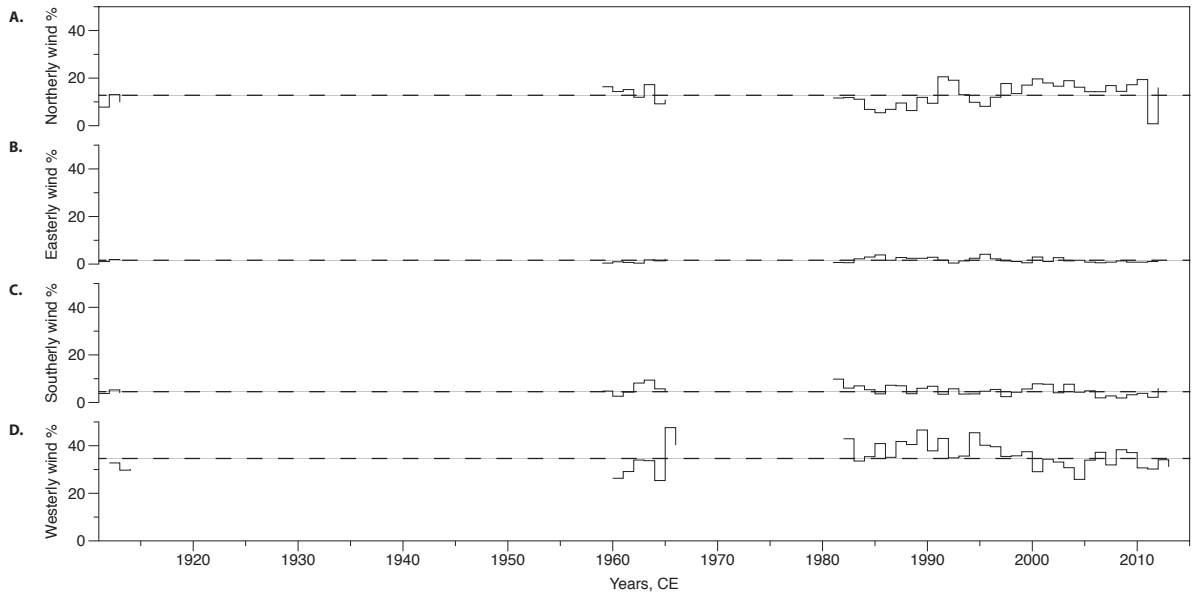

38

39 **Figure S7.** Percentage of austral spring-summer averaged (October-March) wind directions

40 for the four principal meridians over Macquarie Island: northerly (Panel A.), easterly (Panel

41 B.), southerly (Panel C.) and westerly (Panel D.) winds (source: Bureau of Meteorology).

42 Dashed lines denote mean values. Note, no sustained change in wind direction since the

43 Australasian Antarctic Expedition 1912-1915(Newman, 1929).

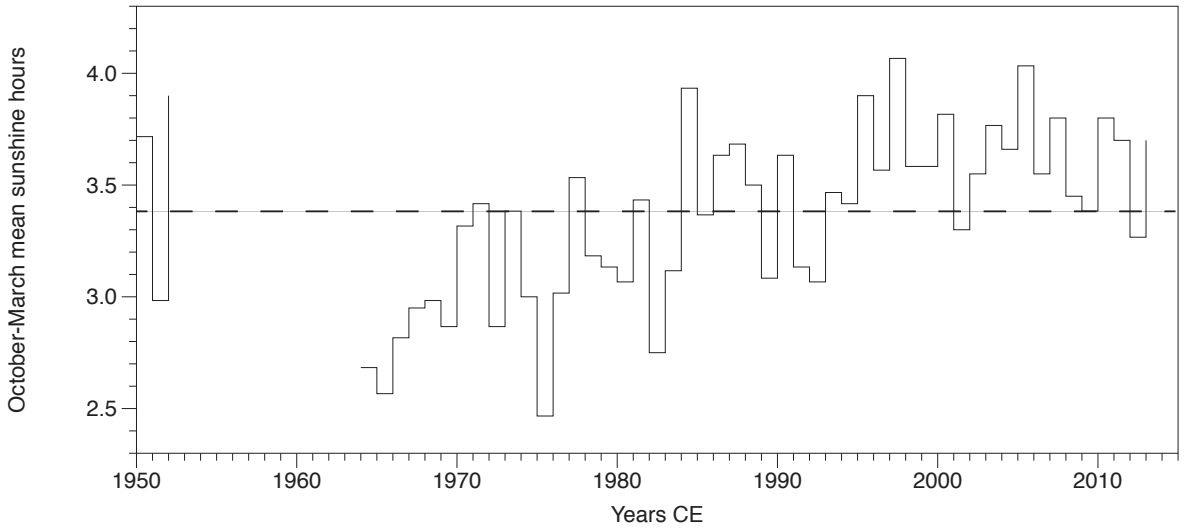

Figure S8. October-March mean daily sunshine hours at Macquarie Island (source: Bureau of Meteorology). Dashed line denotes mean value.

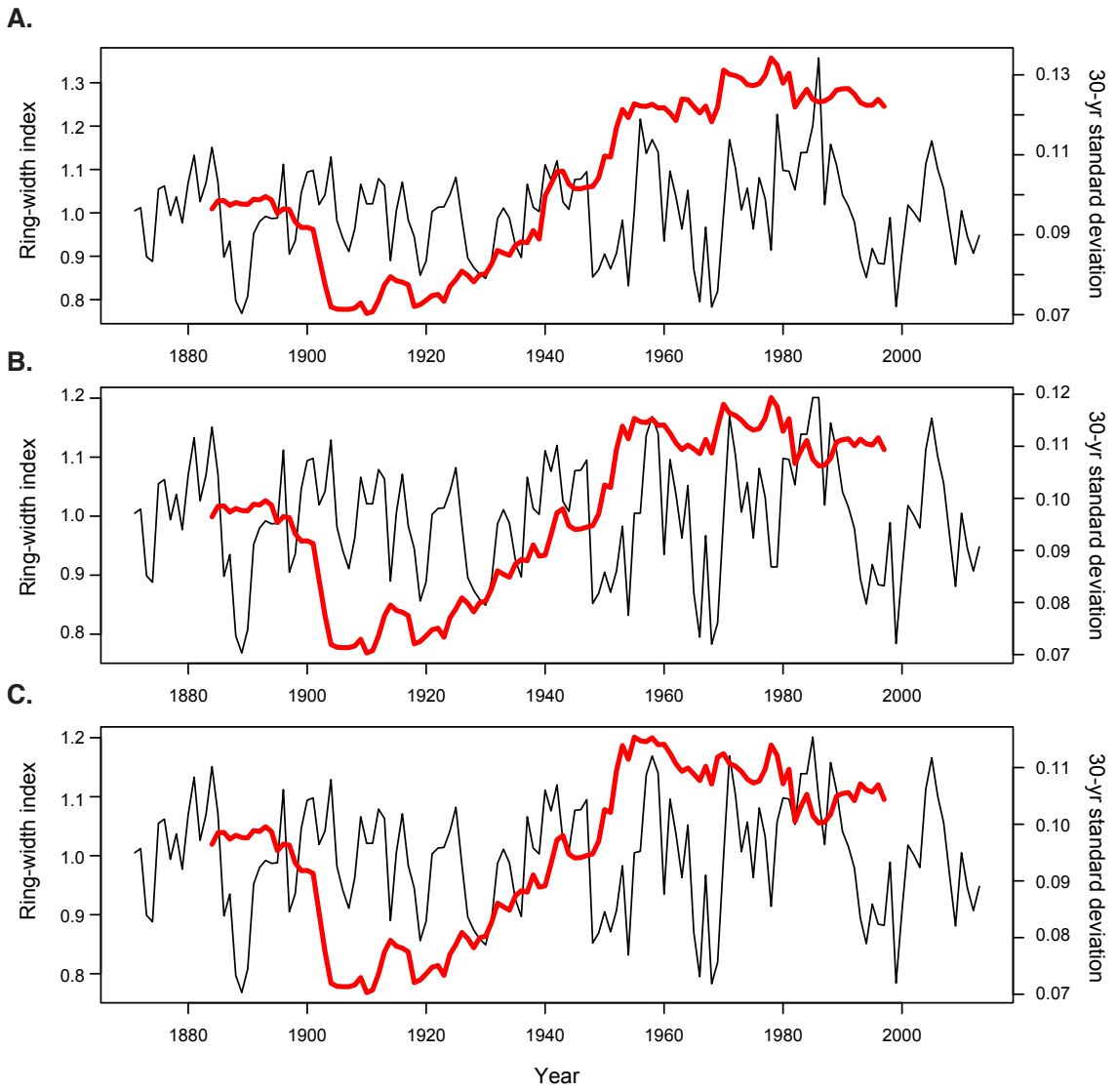

Figure S9: Friedman standardised *Dracophyllum* tree-ring chronology showing original data (black line) and running 30-year standard deviation (red line) (**A.**), values extreme year values from 1956, 1979 and 1986 removed and the previous year's data point duplicated (**B.**), and extreme year values removed and replaced with the decadal average (**C.**). Regardless of the extreme values during 1956, 1979 and 1986, the 30-year standard deviation trend remains the same.

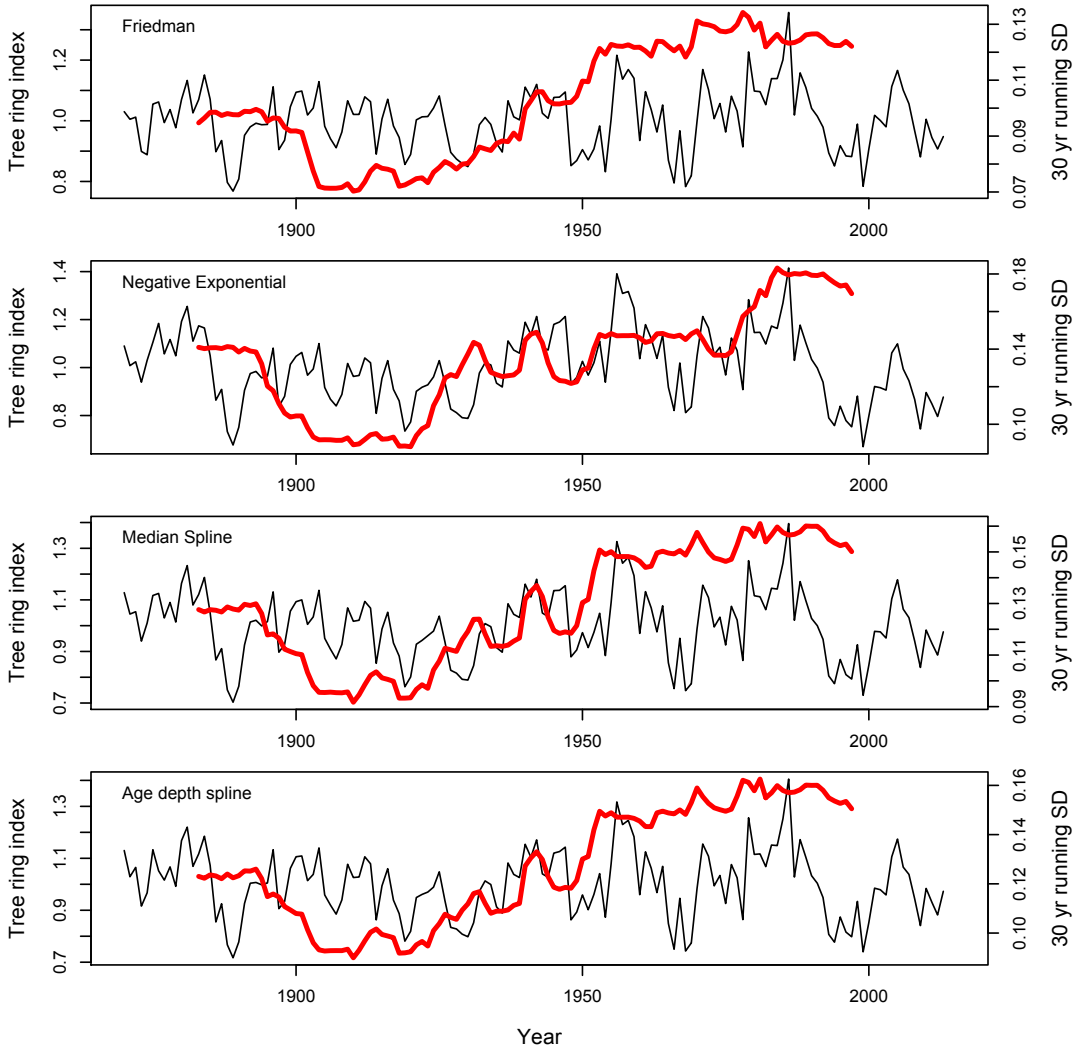

Figure S10: Comparison of the 30-year running standard deviation (red lines) for the different tree-ring index standardisation methods (black lines).

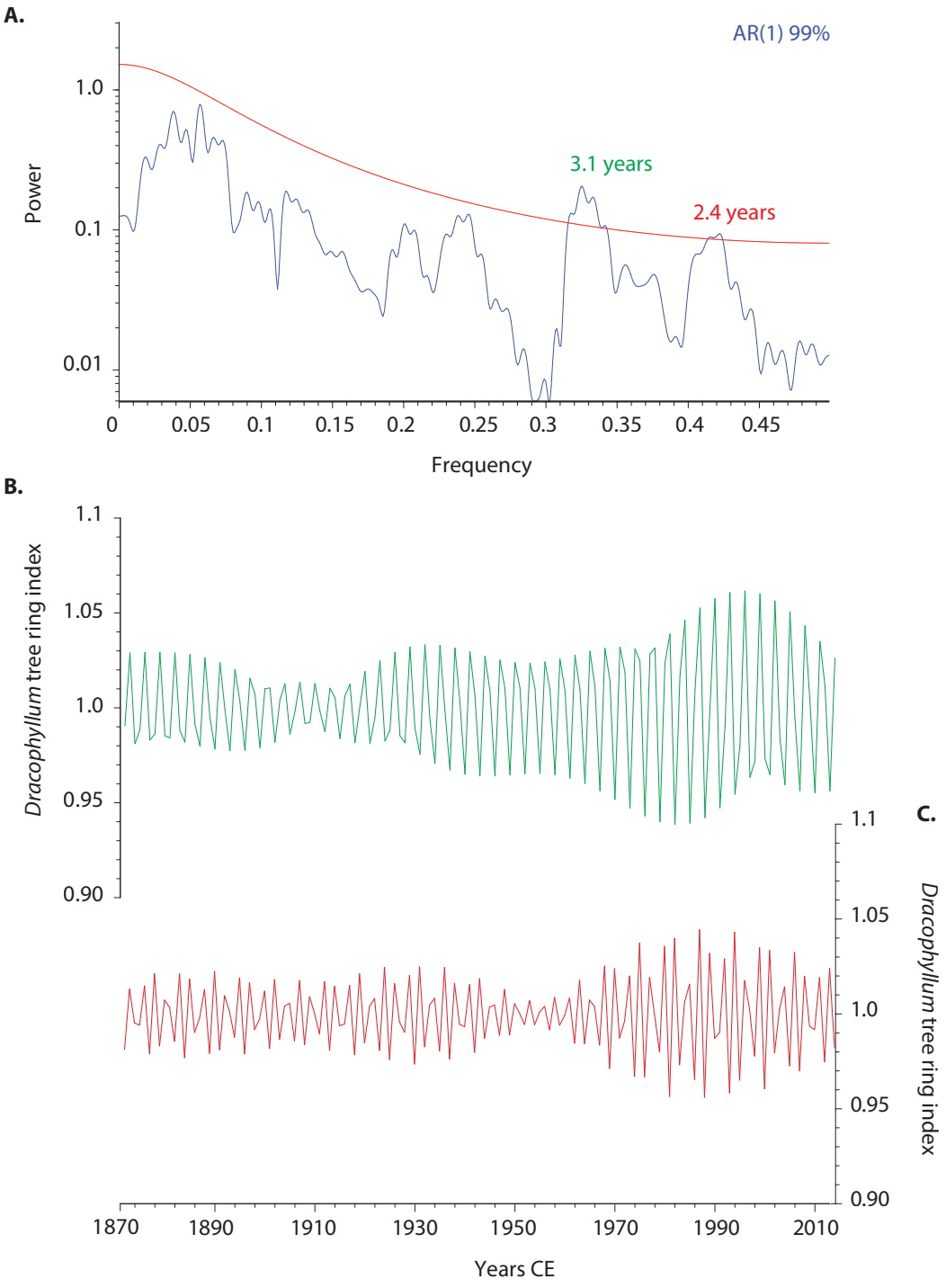

Figure S11: Multi-Taper Method (MTM) (Panel A.) and extracted periodicities exceeding 99% significance (Panels B. and C.) observed in the standardized *Dracophyllum* tree-ring series from Campbell Island since CE 1870.

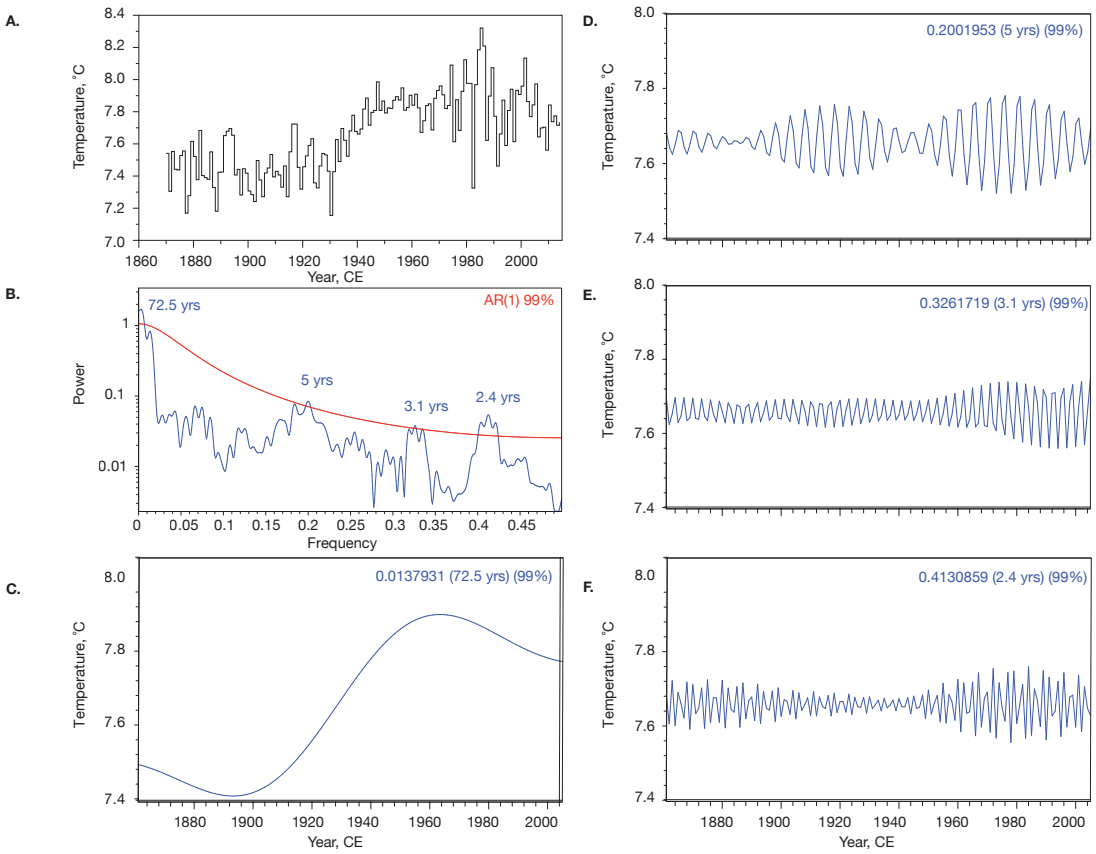

Figure S12: Annual (July-June) southwest Pacific Southern Ocean sea surface temperatures (derived from HadISST) (Rayner et al., 2003) since CE 1870 (Panel A.) with spectral analysis using Multi-Taper Method (MTM) (Panel B.) and extracted climate periodicities exceeding 99% significance (Panels C.-F.).

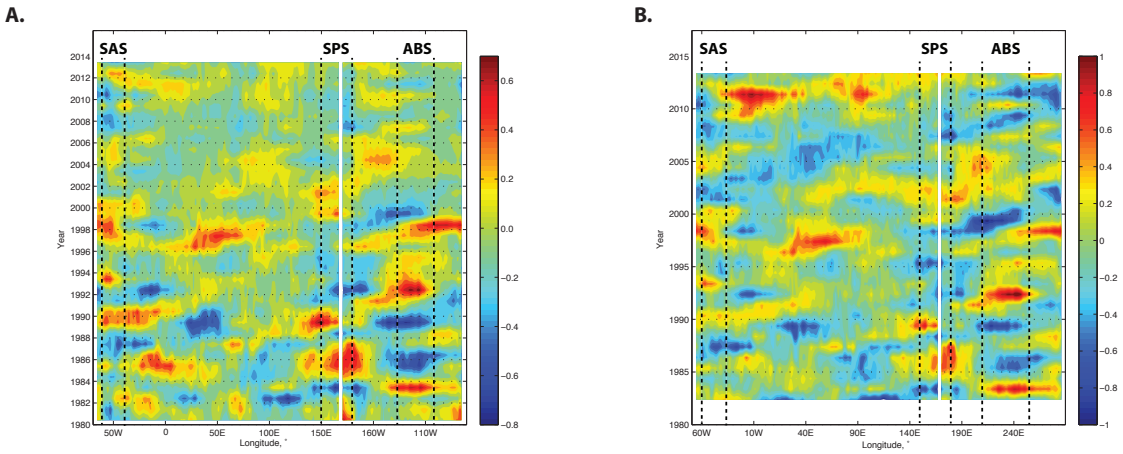

71

72 **Figure S13:** Hovmöller plots showing annual temperature anomaly, meridionally averaged
73 between 45˚ and 55˚S (˚C) using the HadISST (Panel A.) (Rayner et al., 2003) and the
74 Reynolds v2 (Panel B.) (Smith and Reynolds, 2005) SST datasets for the period 1980 to 2014.
75 The longitudes of dominant temperature changes across the southwest Pacific subantarctic
76 islands (SPS), the Amundsen and Bellingshausen seas (ABS) and the south Atlantic
77 subantarctic islands (SAS) are shown.

78

79

80

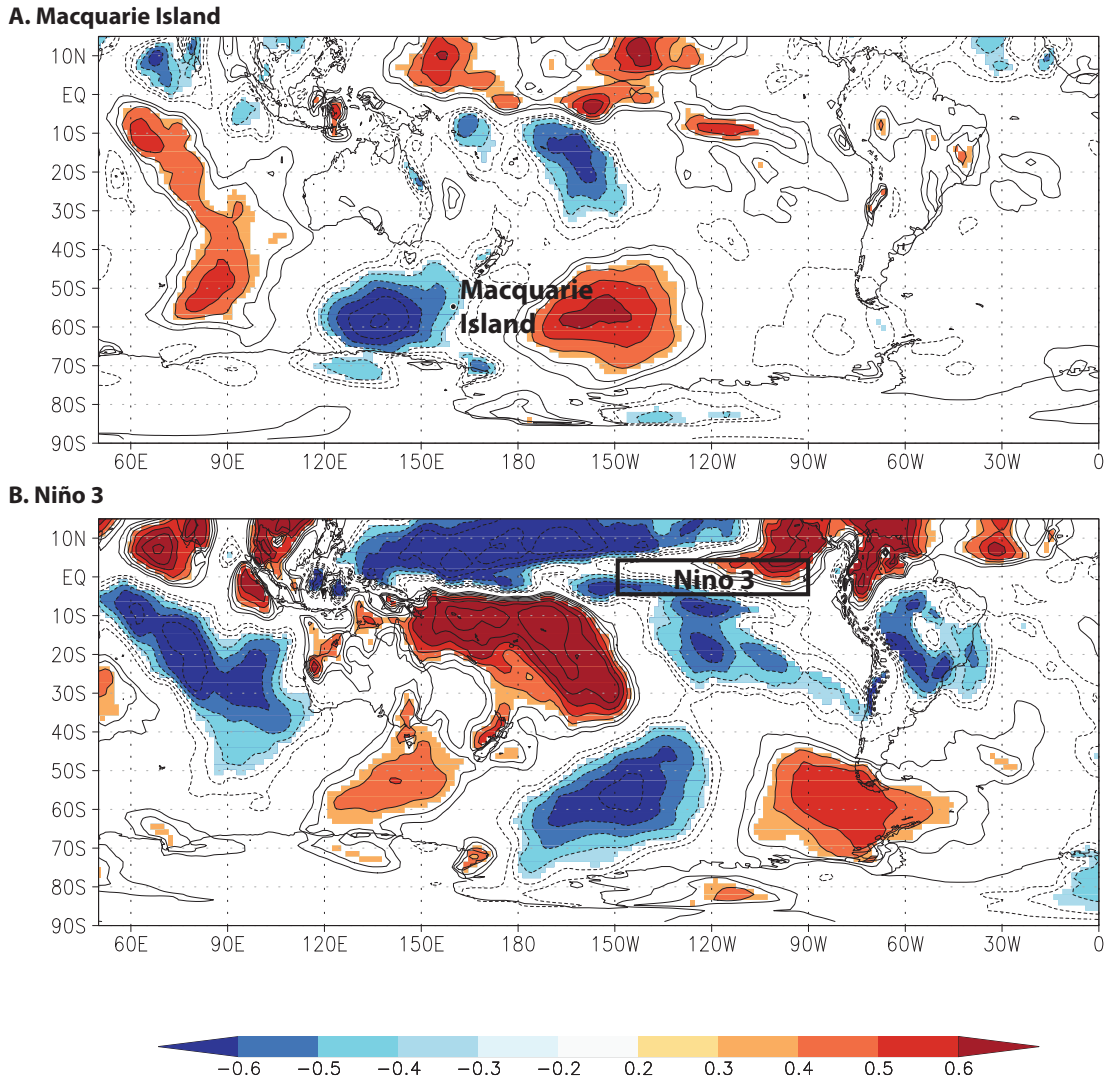

81

82 **Figure S14:** Spatial correlation between deseasonalized and detrended Macquarie Island (**A.**)

83 and Nino 3 (**B.**) (October-March) temperatures and meridional wind stress (850 hPa) (ERA

84 Interim; 1979 to 2013) (Dee et al., 2011). Significance $p_{field} < 0.05$. Note: positive correlations

85 identify regions of enhanced southerly airflow, blue, more northerly airflow.

86

87

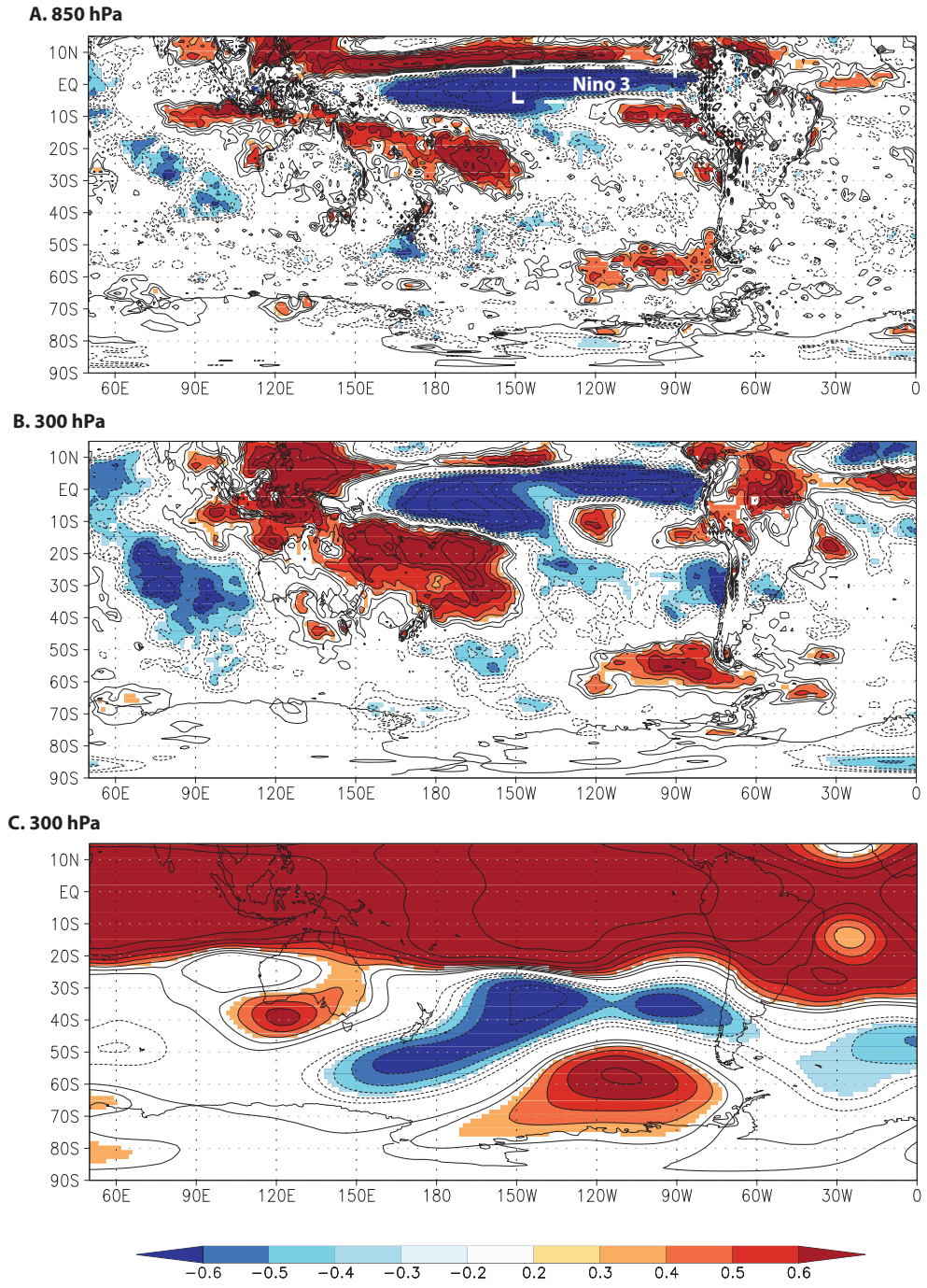

Figure S15: Spatial correlation between detrended and deseasonalised Nino 3 sea surface temperature(Rayner et al., 2003) (October-March) and 850 hPa (**A.**) and 300 hPa (**B.**) vertical velocity and 300 hPa height anomalies (**C.**) using ERA Interim (Dee et al., 2011) for the period 1979-2015. Significance $p_{field} < 0.05$. Note: negative values indicate ascent during warm SST anomalies in Nino 3.

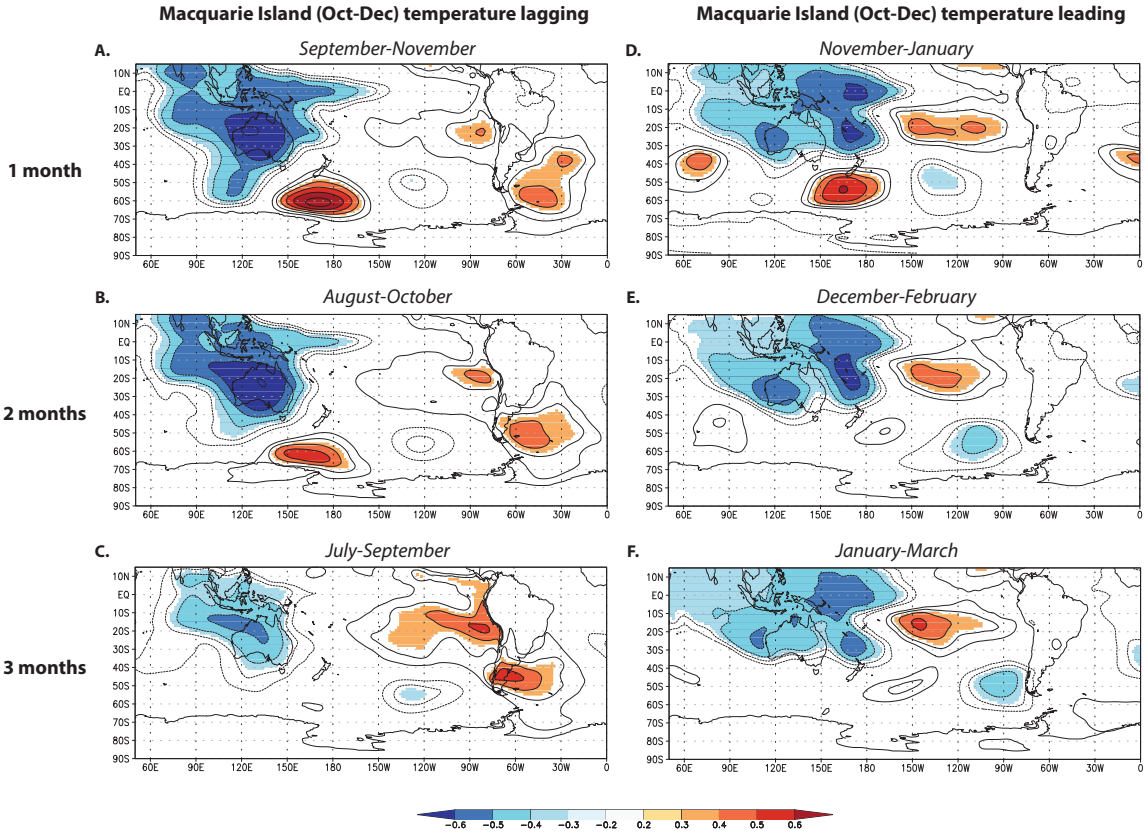

Figure S16: Spatial correlation between detrended and deseasonalised Macquarie Island air temperature (October-December) and 850 hPa height anomalies lagging one (**A.**), two (**B.**) and three (**C.**) months and leading one (**D.**), two (**E.**) and three (**F.**) months using ERA Interim(Dee et al., 2011) for the period 1979-2014. Significance $p_{field} < 0.05$.

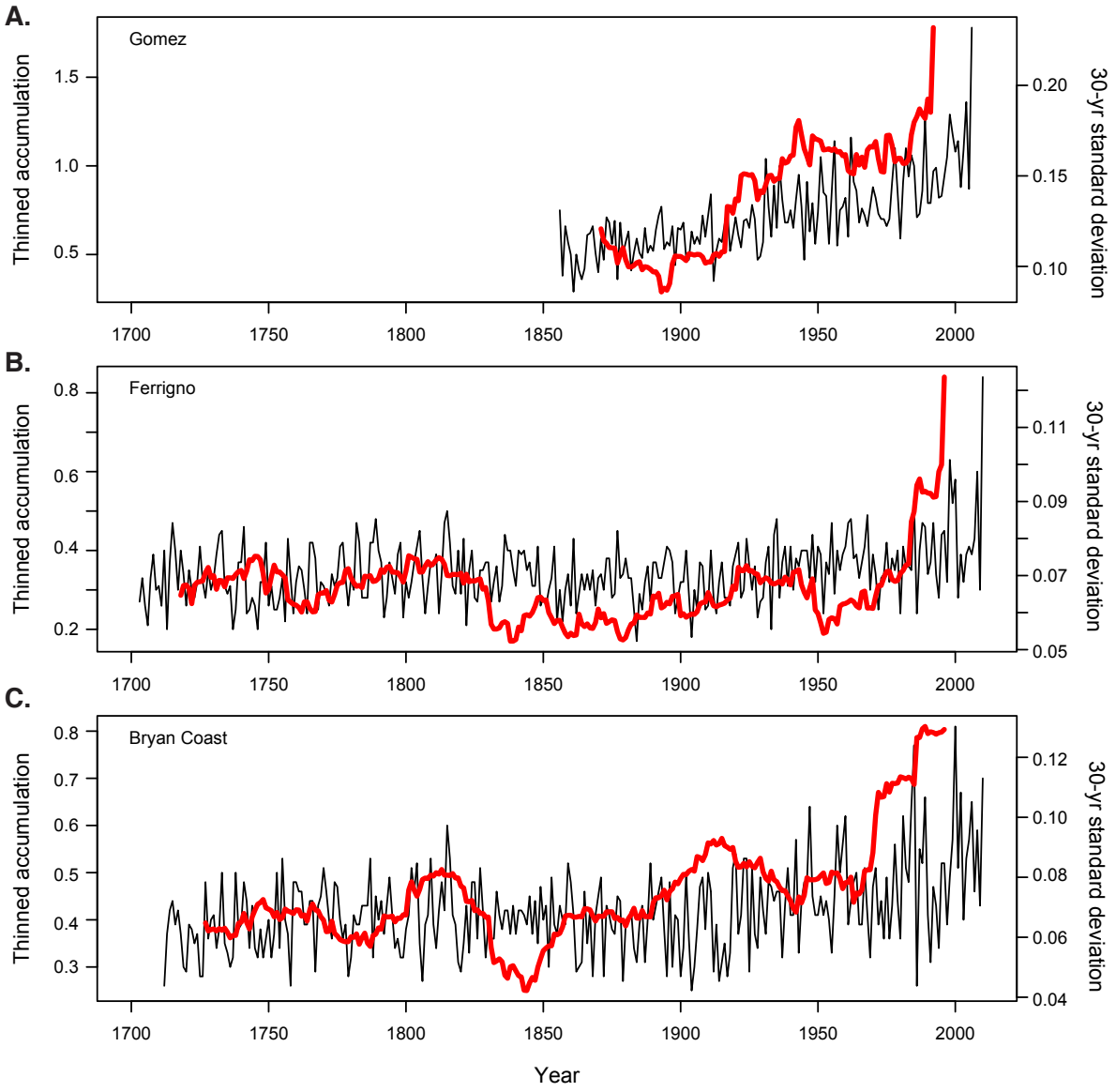

100

101 **Figure S17:** Thinned accumulation in West Antarctic coast ice cores Gomez (**A.**), Ferrigno
102 (**B.**) and Bryan Coast (**C.**) (Thomas et al., 2015; Thomas et al., 2008) with running 30-year
103 mean standard deviation (red line).

	Campbell Island: Observations (#6172)			
	Start	*End*	*Count (days)*	*Percent*
Daily mean sea level pressure	1941-07	1995-08	19719	100
Daily surface wind	1941-07	1995-08	19760	100
Daily air temperature	1941-07	1995-08	19762	100
	Campbell Island: AWS (#6174)			
	Start	*End*	*Count (days)*	*Percent*
Daily mean sea level pressure	1991-10	continuing	9018	100
Daily surface wind	1991-10	continuing	9018	100
Daily air temperature	1991-10	continuing	9025	100
	Macquarie Island			
	Start	*End*	*Count (days)*	*Percent*
Daily mean sea level pressure	1948-05	continuing	24624	98.6
Daily surface wind	1948-05	continuing	24624	98.6
Daily air temperature	1948-05	continuing	24624	98.6

Table S1: Summary of Campbell Island and Macquarie Island climate data including duration of record (year and month) and percentage complete (sources: Bureau of Meteorology and the New Zealand National Climate Database). Stations were inspected and serviced annually. The 'Percent' values provide the completeness of observations averaged over all months of record for the given station and observation type. An automatic weather station (AWS; station number #6174) was installed on Campbell Island in 1990. Sensor and site history of the Campbell Island stations #6172 and #6174 reveal no significant data interruptions. For Macquarie Island the small amount of missing data (1.4%) was mostly during the period CE 1948-1951. No complete months are missing from any of the datasets.

	July	Aug	Sept	Oct	Nov	Dec	Jan	Feb	Mar	April	May	June	Annual
AAE													
1912-1915	2.8	3.1	3.2	3.1	4.3	5.8	6.3	6.1	5.6	4.6	3.8	2.8	4.3
Bureau of Meteorology													
1949-1952	3.3	2.6	3.3	3.4	4.3	6.0	6.5	5.9	5.5	4.7	3.8	2.9	4.4
1953-1956	2.6	3.0	2.7	4.0	4.5	6.2	7.0	6.4	6.0	5.2	4.5	2.9	4.6
1957-1960	2.9	3.3	3.5	3.9	4.6	5.6	6.8	6.8	6.1	5.3	3.7	3.1	4.6
1961-1964	2.8	2.8	3.4	4.1	4.3	5.8	6.4	6.5	5.7	4.8	3.6	3.2	4.4
1965-1968	3.1	3.6	3.5	3.2	4.2	5.5	6.7	6.6	**6.4†**	5.1	4.4	**3.8***	4.7
1969-1972	3.5	3.7	2.5	3.3	4.7	6.2	7.2	**7.2***	6.4	5.1	4.5	3.2	4.8
1973-1976	3.1	3.1	3.7	3.7	4.8	6.7	7.3	**7.1***	6.6	**5.3***	3.7	3.1	**4.8***
1977-1980	**4.3***	**4.0***	3.9	4.1	4.5	6.2	7.4	7.5	**6.8***	**5.7***	4.7	3.7	**5.2†**
1981-1984	3.5	3.3	3.7	4.0	4.6	6.0	6.8	7.0	6.7	5.4	4.6	**3.8***	4.9
1985-1988	3.4	3.5	3.3	4.5	5.2	6.7	**7.9***	**8.0***	6.7	**5.5***	3.8	3.1	**5.1***
1989-1992	3.6	3.3	4.0	4.2	5.0	5.8	7.5	6.9	**6.2***	5.2	4.0	3.6	4.9
1993-1996	2.6	3.2	3.3	3.7	4.6	5.9	6.9	**7.1***	**6.6***	**5.8***	4.6	2.7	4.7
1997-2000	3.6	3.1	4.2	4.0	4.5	6.1	7.0	7.1	6.1	5.0	4.5	3.6	**4.9***
2001-2004	3.6	3.4	3.5	4.1	5.0	6.0	7.4	7.1	**6.5†**	**5.7†**	3.9	3.3	**4.9***
2005-2008	2.9	3.6	3.5	3.8	4.4	6.6	7.1	**7.2***	**6.5†**	**5.8***	4.7	3.3	**4.9***
2009-2012	2.8	3.7	3.8	3.6	3.8	6.1	7.0	**7.0***	**6.4***	**5.8***	4.9	3.2	**4.8***

Table S2: Four-year binned monthly atmospheric temperatures for the Isthmus, Macquarie Island, comparing the record generated from the original Australasian Antarctic Expedition (AAE) with continuous measurements taken since 1949. Statistically-significant two-tailed t-tests are given in bold: *****$p<0.05$ and **†** $p<0.01$.

	July	August	September	October	November	December	January	February	March	April	May	June	Annual
AAE													
1912-1915	3.4	3.6	3.8	4.1	5.1	6.3	6.6	5.7	5.3	4.8	3.9	3.5	4.7
Loewe													
1951-1954	3.6	3.5	3.8	3.8	5.4	6.7	7.3	7.2	6.7	5.8	4.7	3.8	5.2
1957, 1962-1964	4.2	4.2	4.4	4.6	5.4	5.4	7.0	6.7	6.1	5.5	4.7	4.2	5.2
MODIS													
2001-2004	2.9	3.5	3.6	3.9	4.3	5.9	7.1	6.9	**6.8***	5.3	**5.4***	2.7	4.8
2005-2008	2.7	2.7	4.4	3.9	4.6	5.8	6.4	**7.0***	**6.4***	5.8	5.0	3.8	4.9
2009-2012	3.4	4.3	4.1	4.6	4.8	5.8	6.7	**7.5***	**6.9***	5.3	4.3	3.0	5.0

Table S3: Four-year binned monthly sea surface temperature (SST) for Buckles Bay, Macquarie Island, comparing the record generated from the original Australasian Antarctic Expedition with those obtained during the 1950s and 1960s (Loewe, 1968, 1957) and MODIS 4 km-resolved 11 μm daytime satellite observations. Statistically-significant two-tailed t-tests <0.05 denoted by * and given in bold. Note, the 1950s and 1960s SSTs obtained from Macquarie Island are reported as monthly averages across the period of observation, precluding t-tests.

Dracophyllum - Campbell Island temperature (˚C, October-March)

Calibration Period	Variance Explained (%)	Pearson Correlation (r)	RE	Verification Period	Pearson Correlation (r)	RE	CE
"Early" 1949-1980	29.9	0.547	0.299	1981-2012	0.552	0.342	0.245
1st-differenced		0.571	0.285		0.619	0.298	0.297
"Late" 1981-2012	28.4	0.533	0.284	1949-1980	0.562	0.410	0.234
1st-differenced		0.639	0.323		0.542	0.289	0.291
Entire Period (1949-2012)	31.3	0.559	0.291				

Dracophyllum - Macquarie Island temperature (˚C, October-March)

Calibration Period	Variance Explained (%)	Pearson Correlation (r)	RE	Verification Period	Pearson Correlation (r)	RE	CE
"Early" 1949-1980	25.7	0.507	0.257	1981-2012	0.449	0.277	-0.003
1st-differenced		0.534	0.262		0.557	0.234	0.232
"Late" 1981-2012	22.2	0.471	0.222	1949-1980	0.524	0.370	-0.478
1st-differenced		0.571	0.258		0.532	0.283	0.283
Entire Period (1949-2012)	26.4	0.513	0.240				

127

128 **Table S4**: Calibration and verification statistics for the *Dracophyllum* tree-ring reconstruction of 'growing-season' temperature on Campbell

129 and Macquarie islands (October-March).

Tree-ring standardisation	F-test ratio of variances	*p* value	Bartlett's K-squared	*p* value
Friedman temperature reconstruction	0.513	<0.0055	7.7069	<0.0055
Friedman tree-ring index	0.518	<0.0061	7.5294	<0.0061
Medium spline tree-ring index	0.561	<0.0158	5.8285	<0.0158
Negative exponential tree-ring index	0.645	<0.0663	3.3752	<0.0662
Age depth spline tree-ring index	0.601	<0.0333	4.5363	<0.0332

Table S5: Comparison of the variance across the tree-ring record (CE 1870-1940 vs 1941-2012), for different standardization methods and the Friedman temperature reconstruction reported here. The second half of the twentieth century is significantly larger (in all cases F and Bartlett's K-squared tests $p < 0.07$), suggesting a shift in climate to one characterised by pervasive high variability, regardless of the standardisation method used.

CMIP5 model	Correlation to reconstructed Macquarie Island temperature (Oct-Mar)	Significance (*p*)
ACCESS1-0	0.001	0.9946
ACCESS1-3	0.070	0.2561
bcc-csm1-1	0.026	0.6751
bcc-csm1-1-m	-0.027	0.6601
BNU-ESM	-0.054	0.6142
CanESM2	-0.071	0.1412
CCSM4	0.050	0.2574
CESM1-BGC	-0.011	0.9179
CESM1-CAM5	-0.047	0.4531
CESM1-CAM5-1-FV2	-0.088	0.1000
CESM1-FASTCHEM	-0.038	0.5418
CESM1-WACCM	-0.014	0.8975
CMCC-CM	-0.072	0.5002
CMCC-CMS	-0.033	0.7611
CMCC-CESM	-0.134	0.2184
CNRM-CM5	-0.037	0.2770
CSIRO-Mk3-6-0	0.003	0.9271
EC-EARTH	0.002	0.9623
FGOALS-g2	-0.048	0.3097
FIO-ESM	-0.055	0.3747
GFDL-CM3	-0.006	0.8963
GFDL-ESM2G	0.103	0.0958
GFDL-ESM2M	-0.006	0.9584
GISS-E2-H p1	0.022	0.6807
GISS-E2-H p2	0.043	0.3760
GISS-E2-H p3	-0.023	0.6019
GISS-E2-H-CC p1	0.015	0.8915
GISS-E2-R p1	-0.009	0.8338

GISS-E2-R p2	-0.038	0.3843
GISS-E2-R p3	0.008	0.8622
GISS-E2-R-CC p1	0.015	0.8915
HadGEM2-AO	-0.006	0.9555
HadGEM2-CC	-0.067	0.5319
HadGEM2-ES	**-0.114**	**0.0300**
inmcm4	0.065	0.5538
IPSL-CM5A-LR	0.001	0.9793
IPSL-CM5A-MR	-0.032	0.6135
IPSL-CM5B-LR	0.174	0.0891
MIROC5	**0.120**	**0.0097**
MIROC-ESM	0.012	0.8470
MIROC-ESM-CHEM	-0.133	0.2194
MPI-ESM-LR	0.074	0.2269
MPI-ESM-MR	0.009	0.8858
MPI-ESM-P	0.011	0.8866
MRI-CGCM3	-0.090	0.1471
MRI-ESM1	0.069	0.5295
NorESM1-M	0.052	0.6339
NorESM1-ME	0.042	0.4934

Table S6: Correlations and significance between CMIP5 modelled surface air temperatures centred over 52-57˚S and 157-162˚E (Taylor et al., 2011) and reconstructed Macquarie Island temperatures (detrended and deseasonalised October-March, CE 1871-2004). $p < 0.05$ given in bold. Note, HadGEM2-ES is inversely correlated and MIROC5 has a correlation of only 0.12.

	Eastern rockhopper (*Eudyptes filholi)*	Erect crested penguin (*Eudyptes sclateri)*
1978	50,000	115,000
1995	3,392	52,000
2011	2,475	42,689

Table S7: Eastern rockhopper and Erect crested penguin populations on the Antipodes Islands. In 1978 breeding pairs were counted whereas in 1995 and 2011 nests were the unit counted (Hiscock and Chilvers, 2014).

References

Dee, D. P., Uppala, S. M., Simmons, A. J., Berrisford, P., Poli, P., Kobayashi, S., Andrae, U., Balmaseda, M. A., Balsamo, G., Bauer, P., Bechtold, P., Beljaars, A. C. M., van de Berg, L., Bidlot, J., Bormann, N., Delsol, C., Dragani, R., Fuentes, M., Geer, A. J., Haimberger, L., Healy, S. B., Hersbach, H., Hólm, E. V., Isaksen, L., Kållberg, P., Köhler, M., Matricardi, M., McNally, A. P., Monge-Sanz, B. M., Morcrette, J. J., Park, B. K., Peubey, C., de Rosnay, P., Tavolato, C., Thépaut, J. N., and Vitart, F.: The ERA-Interim reanalysis: configuration and performance of the data assimilation system, Quarterly Journal of the Royal Meteorological Society, 137, 553-597, 2011.

Hiscock, J. A. and Chilvers, B. L.: Declining eastern rockhopper (*Eudyptes filholi*) and erect-crested (*E. sclateri*) penguins on the Antipodes Islands, New Zealand, New Zealand Journal of Ecology, 38, 124-131, 2014.

Loewe, F.: A further note on the sea water temperatures at Macquarie Island, Australian Meteorological Magazine, 16, 118-119, 1968.

Loewe, F.: A note on the sea water temperatures at Macquarie Island, Australian Meteorological Magazine, 19, 60-61, 1957.

Marshall, G.: Trends in the Southern Annular Mode from observations and reanalyses, Journal of Climate, 16, 4134-4143, 2003.

Masumoto, Y., Sasaki, H., Kagimoto, T., Komori, N., Ishida, A., Sasai, Y., Miyama, T., Motoi, T., Mitsudera, H., Takahashi, K., Sakuma, H., and Yamagata, T.: A fifty-year eddy-resolving simulation of the world ocean – Preliminary outcomes of OFES (OGCM for the Earth simulator), Journal of the Earth Simulator, 1, 35-56, 2004.

Newman, B. W.: Meteorology. Tabulated and Reduced Records of the Macquarie Island Station, Sydney, 539 pp., 1929.

Rayner, N. A., Parker, D. E., Horton, E. B., Folland, C. K., Alexander, L. V., Rowell, D. P., Kent, E. C., and Kaplan, A.: Global analyses of sea surface temperature, sea ice, and night marine air temperature since the late nineteenth century, Journal of Geophysical Research: Atmospheres, 108, 4407, doi:4410.1029/2002JD002670, 2003.

Sallée, J.-B., Matear, R. J., Rintoul, S. R., and Lenton, A.: Localized subduction of anthropogenic carbon dioxide in the Southern Hemisphere oceans, Nature Geoscience, 5, 579-584, 2012.

Smith, T. M. and Reynolds, R. W.: A global merged land-air-sea surface temperature reconstruction based on historical observations (1880-1997), Journal of Climate, 18, 2021-2036, 2005.

Taylor, K. E., Stouffer, R. J., and Meehl, G. A.: An overview of CMIP5 and the experiment design, Bulletin of the American Meteorological Society, 93, 485-498, 2011.

Thomas, E. R., Hosking, J. S., Tuckwell, R. R., Warren, R., and Ludlow, E.: Twentieth century increase in snowfall in coastal West Antarctica, Geophysical Research Letters, 42, 9387-9393, 2015.

Thomas, E. R., Marshall, G. J., and McConnell, J. R.: A doubling in snow accumulation in the western Antarctic Peninsula since 1850, Geophysical Research Letters, 35, doi: 10.1029/2007GL032529, 2008.